# Synthesis, characterisation and *in situ* colorimetry of electrochromic Ruthenium purple thin films

**Roger J. Mortimer*, Thomas S. Varley**

*Department of Chemistry, Loughborough University, Loughborough, Leicestershire, LE11 3TU, UK*

**Abstract**

Ruthenium purple (RP) films on transmissive tin-doped indium oxide (ITO)/glass substrates have been synthesised by an electrochemical coagulation technique using an aqueous RP colloidal suspension prepared from separate very dilute aqueous solutions of iron(III) chloride and potassium hexacyanoruthenate(II), with dilute potassium chloride as supporting electrolyte solution. To aid stability of the RP films, ruthenium(III) chloride was added to the RP colloidal suspension. Using the CIE (Commission Internationale de l'Eclairage) system of colorimetry, the colour stimulus of the electrochromic RP films and the changes that take place on reversibly switching to the colourless form have been calculated from *in situ* visible spectra recorded under electrochemical control. On electrochemical reduction, the intensely absorbing bright purple mixed-valence iron(III) hexacyanoruthenate(II) chromophore is reduced to the colourless iron(II) hexacyanoruthenate(II) form. Sharp and reversible changes in the hue and saturation occur, as shown by the track of the CIE 1931 *xy* chromaticity coordinates. Concurrently, as the purple chromophore is bleached, a large increase in the relative luminance of the electrochromic film is observed. For the purple state, the CIELAB 1976 colour space coordinates were $L^*$ = 64, $a^*$ = 27 and $b^*$ = -36, with a complementary wavelength ($\lambda_c$) calculated as 555 nm, in excellent agreement with the absorption maximum ($\lambda_{max}$) of 550 nm for the intervalence charge-transfer (IVCT) band.

* Corresponding author. Tel.: +44 1509 222 583; fax: +44 1509 223 925.
*E-mail address*: R.J.Mortimer@lboro.ac.uk (R.J.Mortimer)

*Keywords*: Electrochromic; Electrochromism; Ruthenium purple; CIE chromaticity coordinates; Colorimetry

## 1. Introduction

Prussian blue (PB), the earliest [1] modern synthetic pigment (C.I. Pigment Blue 27), has an extensive history of use in the formulation of paints, lacquers, printing inks, typewriter ribbons and carbon paper [2-4]. The intense colour of the iron(III) hexacyanoferrate(II) chromophore arises from intervalence charge-transfer (IVCT) between the mixed-valence iron oxidation states [5]. PB and numerous other polynuclear metal hexacyanometallates [6], can be deposited onto inert electrode substrates to give redox-active films that have electrochromic properties [7,8]. We have earlier described the application of an *in situ* colorimetric method, based on the CIE (Commission Internationale de l'Eclairage) system of colorimetry, to the study of electrochromism in PB films [9]. We now report the quantification of the colour stimulus in films of the Group 8 PB analogue, Ruthenium purple (RP), and the changes that take place on reversibly switching the intensely absorbing bright purple iron(III) hexacyanoruthenate(II) chromophore to the colourless form, iron(II) hexacyanoruthenate(II).

Although thin-film PB is readily available through electrochemical reduction of solutions containing iron(III) and hexacyanoferrate(III) ions [6-9], synthesis of RP films [10-19] is less straightforward. Salts of the analogous hexacyanoruthenate(III) ion are not commercially available, and although preparation by chemical or electrochemical oxidation of hexacyanoruthenate(II) is possible, the resulting solution is unstable. In the synthetic procedure described here, we employ an electrochemical coagulation technique using an aqueous RP colloidal suspension prepared from separate fresh very dilute solutions of iron(III) chloride and potassium hexacyanoruthenate(II), with dilute potassium chloride as supporting electrolyte. This technique was first introduced by Cataldi et al. [12] and here we provide an explanation of the need to adhere to specific concentrations for reproducible

success in RP film formation and give exact synthetic details for the preparation and use of the colloidal suspension.

## 2. Experimental

*2.1. Materials*

Working electrode substrates were tin-doped indium oxide (ITO) on glass (7 x 50 x 0.7 mm, 5-15 Ω/□, part no. CG-50IN-CUV) from Delta Technologies Limited. Before each RP film formation, ITO/glass substrates were pre-treated, in order to remove any trace of adhesive/impurities on the surface, by sonication (5 minutes) in isopropyl alcohol followed by rinsing with deionised water and air drying. The counter electrode was platinum gauze and the reference electrode was Ag/AgCl (3.0 mol $dm^{-3}$ NaCl). Anhydrous iron(III) chloride, potassium hexacyanoruthenate(II) hydrate, ruthenium(III) chloride, potassium chloride and hydrochloric acid (all Sigma-Aldrich) were of the highest purity available and used without further purification. All deionised water for solution preparation and the resulting electrolyte solutions and colloidal suspensions were deoxygenated by nitrogen purging for 20 min prior to all measurements.

*2.2. Electrochemical and spectroelectrochemical measurements*

An ECO Chemie Autolab PGSTAT 20 potentiostat was used for electrode potential control, with *in situ* visible region spectra being recorded using a Hewlett Packard 8452A diode array spectrophotometer. A single-compartment glass electrochemical cell was used for electrochemical deposition and cyclic voltammetric characterisation of RP films. For *in situ* spectroelectrochemistry, a 1 cm pathlength plastic cuvette was used, with a machined polytetrafluoroethylene lid that allowed the ITO/glass working electrode to be mounted parallel to the optical faces. Additional holes in the lid allowed for the counter and reference electrodes to be positioned in the electrolyte solution, and nitrogen purging prior to measurements. The lower 4 cm of each ITO/glass substrate was immersed in solution, providing a submerged geometric electrode active area of 2.80 $cm^2$. Adhesive copper tape

at the top of each ITO/glass substrate provided the means for a uniform electrical contact. In the computation of CIE 1931 chromaticity coordinates, the spectral power distribution of the $D_{55}$ light source was used.

*2.3. Crystallographic and morphological studies*

Powder X-ray diffraction (XRD) analysis of RP films on ITO/glass substrates was carried out with a Bruker D8 Advance diffractometer, using monochromatic CuK α1 radiation at $\lambda$ = 1.5406 Å and a position sensitive detector (PSD). Perspex flat plate sample holders were used to mount the samples and data were collected between the $2\theta$ range of 5-90°, using 0.014767° steps over a period of 4 h.

Scanning electron micrographs (SEM) were produced on a Carl Zeiss 1530 VP Field Emission Gun Scanning Electron Microscope (FEG-SEM) with an EDAX Phoenix energy dispersive X-ray microanalysis system.

A Malvern Zetamaster ZEM5002 colloid analyser was used to determine the particle size distribution of colloidal RP present in the deposition solution. The instrument was calibrated using Nanosphere™ size standards (220 ± 6 nm), which gave a mean measurement of 220.7 nm (over ten measurements). The zeta potential of the deposition solution was measured using the same instrument and calibrated using a zeta potential transfer standard (−50 ± 5 mV), which gave a mean reading of 52.3 mV (over ten measurements).

*2.4. Preparation of a dilute colloidal suspension of Ruthenium purple*

An aqueous solution of 1 mmol $dm^{-3}$ potassium hexacyanoruthenate(II) was first prepared by dissolution of potassium hexacyanoruthenate(II) hydrate powder in deoxygenated water (25 $cm^3$) that contained 35 mmol $dm^{-3}$ potassium chloride. A separate aqueous solution containing 1 mmol $dm^{-3}$ iron(III) chloride was next prepared by dissolution of high purity (>99.99%) anhydrous iron(III) chloride powder in deoxygenated water (25 $cm^3$) that contained 35 mmol $dm^{-3}$ potassium chloride. The two freshly prepared

solutions were then rapidly mixed with vigorous stirring to yield a brilliant-purple opaque RP dilute colloidal suspension, which was then adjusted to pH 2 by the addition of hydrochloric acid. Under ultrasonic agitation and further nitrogen purging, 1 $cm^3$ of a 1 mmol $dm^{-3}$ aqueous ruthenium(III) chloride solution was added to the suspension by pipette, to give 0.02 mmol $dm^{-3}$ ruthenium(III) chloride. It was essential to use the RP dilute colloidal suspension within circa four hours, after which time particles start to irreversibly coagulate and collect at the bottom of the container.

## 3. Results and discussion

*3.1. Reproducible synthesis and characterisation of Ruthenium purple films*

RP films on ITO/glass were synthesised by adaptation of a literature method [12]. Using the procedure described above (section *2.4*), RP was first prepared as a dilute colloidal suspension by mixing separate aqueous solutions containing low concentrations of equimolar iron(III) chloride and potassium hexacyanoruthenate(II) in potassium chloride supporting electrolyte. On mixing of the reagent solutions, water molecules coordinated to the $Fe^{III}$ ions are displaced by nitrogen atoms from the hexacyanoruthenate(II) ions to generate an extended RP framework based on a face-centred cubic unit cell with $Fe^{III}$–CN–$Ru^{II}$ bridges [20,21]. Under the described experimental conditions, the dilute RP colloidal suspension had a uniform particle size distribution (Fig. 1) with a mean particle size of 8.3 nm, and remained below the critical coagulation concentration (CCC) for up to four hours. The mean zeta potential value of −22.81 mV (over ten measurements) was indicative of the incipient instability of the dilute RP colloidal suspension.

To achieve reproducible RP films it was essential to exactly follow the procedure detailed above, which was established following extensive explorative work. If not exactly followed, synthesised RP films are often non-adherent, and irreproducible cyclic voltammograms are obtained during RP film growth and subsequent redox cycling. Preparation of separate dilute reagent solutions, followed by rapid mixing with vigorous

stirring was essential and prevented further growth of nuclei and irreversible bulk coagulation. To allow continuous RP film growth, the supporting electrolyte ionic strength was prepared as < 40 mmol $dm^{-3}$ (when using KCl). Higher ionic strengths of supporting electrolyte salt causes irreversible bulk coagulation of the RP hydrophobic sol.

Following RP film synthesis, it is well known that subsequent redox cycling in a $Ru^{III}$-containing solution (pH 2) yields extremely stable ruthenium-modified RP films [12,13], with extensive cross-linking between hydrated RP particles through dinuclear [Fe, Ru] oxo and cyanide bridges [22]. In the present work, the procedure has been simplified, by the inclusion of 0.02 mmol $dm^{-3}$ ruthenium(III) chloride, which allows stabilised RP film formation *from a single dilute colloidal suspension*. Higher ruthenium(III) chloride concentrations caused irreversible bulk coagulation of the RP. Once transferred to the electrochemical cell, the electrode potential was held at +0.60 V for 5 s and then cycled, +0.60 V → −0.20 V → +0.60 V (*vs*. Ag/AgCl (3.0 mol $dm^{-3}$ NaCl)), *n* times (typically 50) at 50 $mVs^{-1}$ (Fig. 2), to obtain firm, adherent RP films, with excellent colour uniformity across the electrode area. The wider potential range used earlier [12] (−0.30 V → +1.00 V *vs*. SCE) was not required.

On transfer to 40 mmol $dm^{-3}$ potassium chloride supporting electrolyte solution and reversible cycling between RP and the colourless redox state (iron(II) hexacyanoruthenate(II)), the surface-confined pigment showed the expected linear dependence of peak current on scan rate (Fig. 2). With ruthenium(III) chloride inclusion in the single dilute colloidal suspension, the resulting RP film degraded to less than 1% of peak current after 200 redox cycles to the colourless form. In the absence of ruthenium(III) chloride, the RP film degraded within 20 cycles.

The voltammetric reduction wave has two peaks, whereas the oxidation process only has one (Fig. 2). Reaction order measurements showed the $K^+$ concentration dependence to be Nernstian (59.2 mV $decade^{-1}$) over four orders of magnitude (4.2 x $10^{-4}$

to 4.2 mol $dm^{-3}$ potassium chloride), potassium ions intercalating/de-intercalating on RP reduction/oxidation. These measurements showed the second reduction peak to disappear at high $K^+$ concentration, indicating that the double reduction wave is a result of two charge compensation processes. The negative charge of the extra electron from the $Fe^{III}$ reduction is balanced by either interstitial $Fe^{III}/Ru^{III}$ or intercalating potassium ions, each process having a slightly different peak potential.

The structure of the RP as a film on ITO/glass substrates was confirmed by X-ray powder diffraction pattern analysis. The peaks at 17.0° (200), 24.5° (220), 34.1°(400), and 44.8° (420) are in close agreement with those found for bulk synthesis of RP powder in the present work and from the literature [19]. The RP can be indexed as a face-centred cubic structure and belongs to the space group *Fm3m* [19]. Scanning electron microscopy (Fig. 3) of the RP films showed a uniform distribution of sub-micron sized particles across the ITO/glass substrate, with an average film thickness of 100 nm, as calculated from the 1.85 mC $cm^{-2}$ charge passed on electrochemically switching colour states.

*3.2. Spectroelectrochemistry and colour stimulus measurement*

*3.2.1. Spectroelectrochemistry of RP films*

Using the synthetic methodology described here, RP film thickness and colour intensity is scalable through the number of electrode potential cycles in the dilute aqueous RP colloidal suspension. For spectroelectrochemical and colour stimulus measurement studies, to enhance contrast on reversibly switching to the colourless form, 100 cycles were now implemented (Fig. 4), with the cyclic voltammetric response and *in situ* spectral measurements of the RP film in supporting electrolyte solution being given in Fig. 5. The iron(III) hexacyanoruthenate(II) chromophore in RP exhibits the expected broad IVCT band, with an absorption maximum ($\lambda_{max}$) at circa 550 nm, the average human eye perceiving the colour as bright purple. The IVCT band in the iron(III) hexacyanoruthenate(II) chromophore is at a lower wavelength than that for iron(III)

hexacyanoferrate(II) in PB, which is attributed to the relative ease with which an electron may be transferred from the $nd^6$ metal ions to the $Fe^{III}$ common acceptor in Group 8 iron(III) hexacyanometallates [5].

*3.2.2. Colorimetric analysis*

RP colour and the changes that take place on reversibly switching to the colourless form were quantified using CIE principles. Colour [23,24] is a subjective phenomenon, however, much effort has been given to the development of *colorimetric analysis*, which allows a quantitative description of colour and relative transmissivity as sensed by the human eye. Colorimetry provides a more precise way to define colour than qualitatively interpreting spectral absorption bands [25]. In colorimetry the human eye's sensitivity to light across the visible region is measured and a numerical description of the colour stimulus is given. There are three attributes that are used to describe colour. The first identifies a colour by its location in the spectral sequence, *i.e.*, what wavelength is associated with the colour. This is known as the hue, dominant wavelength, or chromatic colour, and is the wavelength where maximum contrast occurs. The second attribute, relating to the level of white and/or black, is known as saturation, chroma, tone, intensity, or purity. The third attribute is the brightness of the colour, also referred to as value, lightness, or luminance. Luminance is very informative in considering the properties of electrochromic materials, because, with only one value, it provides information about the perceived transparency of a sample over the entire visible range.

*3.2.3. CIE colour theory*

In the present work, chromaticity coordinates were calculated using a computer spreadsheet from the spectra shown in Fig. 5. The human eye's cones' spectral responses are known as *l*, *m*, *s* (long, medium and short) and are linear combinations of the colour matching functions, $\bar{x}, \bar{y}$ and $\bar{z}$, as used for a CIE 1931 2° Standard Observer. The mathematical relationships between the CIE tristimulus values *X*, *Y* and *Z* and the colour

matching functions are given by equations (1–3), where $I(\lambda)$ is the normalised spectral power distribution, and $\lambda$ is the wavelength.

$$X = \int_{300}^{780} I(\lambda)\,\bar{x}(\lambda)\,\mathrm{d}\lambda \tag{1}$$

$$Y = \int_{300}^{780} I(\lambda)\,\bar{y}(\lambda)\,\mathrm{d}\lambda \tag{2}$$

$$Z = \int_{300}^{780} I(\lambda)\,\bar{z}(\lambda)\,\mathrm{d}\lambda \tag{3}$$

The CIE recommends that the integration can be carried out by discrete numerical summation, and such computation is straightforward when using a computer spreadsheet:

$$X = \sum_{\lambda} I(\lambda)\,\bar{x}(\lambda)\,\Delta\lambda \tag{4}$$

$$Y = \sum_{\lambda} I(\lambda)\,\bar{y}(\lambda)\,\Delta\lambda \tag{5}$$

$$Z = \sum_{\lambda} I(\lambda)\,\bar{z}(\lambda)\,\Delta\lambda \tag{6}$$

The normalised spectral power distribution of the sample $I(\lambda)$ is related to the un-normalised spectral power distribution of the sample $\phi(\lambda)$ by the equation

$$I(\lambda) = k\,\phi(\lambda) \tag{7}$$

where the normalising constant $k$ is

$$k = 1/\sum_{\lambda} \phi(\lambda)\,\Delta\lambda \tag{8}$$

The definition of the spectral power distribution $\phi(\lambda)$ depends upon whether the analysed light is viewed by reflection or transmission. If viewed by reflection then

$$\phi_{\mathrm{R}}(\lambda) = \rho(\lambda)\,S(\lambda) \tag{9}$$

and if viewed by transmission then

$$\phi_{\mathrm{T}}(\lambda) = \tau(\lambda)\,S(\lambda) \tag{10}$$

In the above equations, $\rho(\lambda)$ is the ideal spectral reflectance, $\tau(\lambda)$ is the ideal spectral transmittance, and $S(\lambda)$ is the spectral power distribution of the light source, which must be specified. If $S(\lambda) = 1$, the light source is also ideal *i.e.*, the light source has the same output

at all wavelengths. Although chromaticity coordinates can be calculated from reflectance measurements, the spectral data here are all from transmission measurements, therefore, all following calculations will involve and refer to transmission (Equation (10)).

From the experimental transmittance measurements, and with knowledge of the spectral power distribution of the light source, the tristimulus values *X*, *Y* and *Z* of the colour are calculated. For colour representation in 2-D space, the tristimulus values are converted to *chromaticity coordinates* (*x*, *y*, *z*) by the following equations

$$x = \frac{X}{X+Y+Z} \tag{11}$$

$$y = \frac{Y}{X+Y+Z} \tag{12}$$

$$z = \frac{Z}{X+Y+Z} = 1 - x - y \tag{13}$$

Finally, the luminance factor $Y_L$ is defined as the ratio of the luminance of the transmitter ($Y$) to that of a perfect transmitter ($Y_0$) under the same conditions.

$$Y_L = \frac{Y}{Y_0} \tag{14}$$

*3.2.4. Colorimetric analysis of the RP electrochromic system*

Table 1 shows *xy* coordinates and the % colorimetric luminance (%$Y_L$) calculated from the spectra in Fig. 5. At the initial +0.60 V applied potential, the stable oxidation state is the bright purple RP iron(III) hexacyanoruthenate(II) chromophore. At this potential the colour is at its most saturated. As the potential is swept in the negative direction, the saturation of the purple colour decreases, as shown by the increase in both the *x* and the *y* values. At the −0.20 V potential limit, the fully colourless iron(II) hexacyanoruthenate(II) oxidation state is reached, at which point the coordinates are coincident with those of the chosen illumination source (the 'white point', where here $x = 0.332$, $y = 0.347$, and % $Y_L$ = 100), full transparency having been reached. On potential direction reversal from −0.20 V,

the colour change is reversed, with near coincidence of chromaticity coordinates at the same potentials coming from each direction.

Fig. 6 (a) shows *xy* data from Table 1 presented as a hue and saturation track in a chromaticity diagram. In Fig. 6 (a) (and Fig. 6 (b)), only selected values from Table 1 are shown, due to the coincidence of data at several of the potentials. Although the *xy* chromaticity diagram is not a uniform colour space, abrupt changes in colour are found to correspond with significant changes in the *xy* coordinates. The changes in *xy* coordinates in Fig. 6 (a) occur as the bright purple iron(III) hexacyanoruthenate(II) is reduced to the colourless iron(II) hexacyanoruthenate(II) redox state. In Fig. 6 (b), the *xy* data from Fig. 6 (a) are overlaid onto the CIE 1931 colour space template, showing the track of the *xy* coordinates between the purple and white (colourless) colour states. In this representation, the line surrounding the horse-shoe shaped area is called the spectral locus, giving the visible light wavelengths. The most saturated colours lie along the spectral locus. The line connecting the longest and shortest wavelengths contains the non-spectral purples and is known as the purple line. Surrounded by the spectral locus and the purple line is the region known as the colour locus, which contains every colour that can exist. The location of any point in the *xy* diagram gives the hue and saturation of the colour. For a given sample, the hue is determined by drawing a straight line through the point representing 'white' and the point of interest to the spectral locus, thus obtaining the dominant wavelength of the colour. For placing a wavelength dependence on the RP purple colour state, which is found along the purple line, a complementary wavelength ($\lambda_c$) can be found by drawing a straight line from the sample coordinates through the white point to the spectral locus. The construction shown in Fig. 6 (b) allows an estimated value of 555 nm, in excellent agreement with the wavelength of maximum absorbance ($\lambda_{max}$) in the visible region spectra (Fig. 5).

In CIE theory colours cannot be specifically associated with a given pair of *xy* coordinates, because the third dimension of colour, lightness, is not included in the

diagram. The relative lightness or darkness of a colour is very important in how it is perceived, and is presented as the relative luminance, $Y$, of the sample, to that of the background, $Y_0$ (equation (14)). Relative luminance values can range from 100% for white samples (no light absorbed) to zero for samples that absorb all the light. Fig. 7 shows in graphical form the dramatic changes on redox switching of the % colorimetric luminance ($\%Y_L$) of the RP system and the good correlation with electrical charge data as determined through integration of the current in the cyclic voltammogram in Fig. 5.

Also shown in Table 1 are the calculated $L^*a^*b^*$ coordinates, a uniform colour space (CIELAB) defined by the CIE in 1976. $L^*$ is the lightness variable of the sample, while $a^*$ and $b^*$ correspond to the two antagonistic chromatic processes (red-green and yellow-blue). In the $L^*a^*b^*$ chromaticity diagram, + $a^*$ is the red direction, – $a^*$ is the green direction, + $b^*$ is the yellow direction, and – $b^*$ is the blue direction. The centre (0, 0) of the chromaticity diagram is achromatic; as $a^*$ and $b^*$ values increase, the saturation of the colour increases. At the initial +0.60 V applied potential, the stable oxidation state is the bright purple RP iron(III) hexacyanoruthenate(II) chromophore. At this potential the colour is at its most saturated, the purple being quantified as a composite of positive (towards red) $a^*$ and negative (towards blue) $b^*$ values. As the potential is swept in the negative direction, the saturation of the purple colour decreases, $a^*$ and $b^*$ values becoming less positive and less negative respectively. Although $L^*a^*b^*$ coordinates are useful for comparing electrochromic colour states it must be appreciated that colorimetric properties will vary as a function of the film thickness and morphology [26]. For the RP electrochromic system, with increase in film thickness there is no significant change in the purple hue, although the colour saturation increases and the luminance decreases. The difference between the luminance values of the RP coloured and colourless states increases with film thickness.

## Conclusion

An electrochemical coagulation technique has been employed for the synthesis of electrochromic Ruthenium purple (RP) films. Successful film formation depends on the use of a dilute RP colloidal suspension, carefully prepared to be below the critical coagulation concentration (CCC). Using a calculation method based on the integration of experimental spectral power distributions derived from *in situ* visible region spectra over the CIE 1931 colour-matching functions, RP film colour stimulus, and the changes that take place on reversibly switching to the colourless form have been calculated.

## Acknowledgements

We thank Loughborough University and the departmental EPSRC Doctoral Training Grant for provision of a research studentship to TSV. We acknowledge Jenna L. Crisp for assistance with the XRD analysis and Sneh Lata Jain for assistance with the characterisation of the RP colloidal suspension.

## References

[1] Diesbach (1704) cited in Gmelin, Handbuch der anorganischen chemie, Frankfurt and Main: Deutsche Chemische Gesellschaft; 1930. vol. 59. Eisen B. p. 671.

[2] Fukuda K. In: Lewis PA, editor. Pigment handbook. vol. I. 2nd. edn. New York: Wiley Interscience; 1988. pp. 357–65.

[3] Colour index. 3rd. edn. vol. 4. The Society of Dyers and Colourists. Bradford, England. 1971. p. 4673.

[4] Colour index international. Pigments and solvent dyes. The Society of Dyers and Colourists. Bradford. England. 1997. pp. 154–155.

[5] Robin MB. The color and electronic configurations of Prussian blue. Inorg Chem 1962;1:337–42.

[6] Itaya K, Uchida I, Neff VD. Electrochemistry of polynuclear transition metal cyanides: Prussian blue and its analogues. Acc Chem Res 1986;19:162–8.

[7] Monk PMS, Mortimer RJ, Rosseinsky DR. Electrochromism: fundamentals and applications. Weinheim: VCH; 1995. ch. 6.

[8] Monk PMS, Mortimer RJ, Rosseinsky DR. Electrochromism and electrochromic devices. Cambridge: Cambridge University Press; 2007. ch. 8.

[9] Mortimer RJ, Reynolds JR. *In situ* colorimetric and composite coloration efficiency measurements for electrochromic Prussian blue. J Mater Chem 2005;15:2226–33.

[10] Itaya K, Ataka T, Toshima S. Electrochemical preparation of a Prussian blue analogue: Iron-ruthenium cyanide. J Am Chem Soc 1982;104:3751–2.

[11] Rajan KP, Neff VD. Electrochromism in the mixed-valence hexacyanides. 2. Kinetics of the reduction of Ruthenium purple and Prussian blue. J Phys Chem 1982;86:4361–8.

[12] Cataldi TRI, de Benedetto GE, Campa C. Electrochemical quartz crystal microbalance study and electrochromic behavior of a novel ruthenium purple film. J Electroanal Chem 1997;437:93–8.

[13] Cataldi TRI, De Benedetto GE. On the ability of ruthenium to stabilize polynuclear hexacyanometallate film electrodes. J Electroanal Chem 1998;458:149–54.

[14] Kasem KK. Electrochemical behavior of iron-hexacyanoruthenate(II) thin films in aqueous electrolytes: potential analytical and catalytic applications. Mater Sci Eng B 2001;83:97–105.

[15] Abe T, Toda G, Tajiri A, Kaneko M. Electrochemistry of ferric ruthenocyanide (Ruthenium purple), and its electrocatalyis for proton reduction. J Electroanal Chem 2001;510:35–42.

[16] Millward RC, Madden CE, Sutherland I, Mortimer RJ, Fletcher S, Marken F, Directed assembly of multilayers – the case of Prussian blue. Chem Commun 2001;1994–5.

[17] Sone K, Yogi M. Spectrocyclic voltammetry of Ruthenium purple electrodeposited on a $WO_3$/tris(2,2´-bipyridine)-ruthenium(II)/polymer hybrid film. Macromol Symp 2006;235:179–86.

[18] Tian F, Llaudet E, Dale N. Ruthenium purple-mediated microelectrode biosensors based on sol-gel film. Anal Chem 2007;79:6760–6.

[19] Jain V, Sahoo R, Jinschek JR, Montazami R, Yochum HM, Beyer FL, et al. High contrast solid state electrochromic devices based on Ruthenium Purple nanocomposites fabricated by layer-by-layer assembly. Chem Commun 2008;3663–5.

[20] Keggin JF, Miles FD. Structures and formulae of the Prussian blues and related compounds. Nature (London) 1936;137:577–8.

[21] Inoue H, Yanagisawa S. Bonding nature and semiconductivity of Prussian blue and related compounds. J Inorg Nucl Chem 1974;36:1409–11.

[22] De Benedetto GE, Guascito MR, Ciriello R, Cataldi TRI. Analysis by x-ray photoelectron spectroscopy of ruthenium stabilised polynuclear hexacyanometallate film electrodes. Anal Chim Acta 2000;410:143–52.

[23] Christie RM. Colour chemistry, Cambridge: Royal Society of Chemistry; 2001. ch. 2.

[24] Kuehni RG. Color: an introduction to practice and principles. 2nd edn. Hoboken. New Jersey: J. Wiley & Sons; 2005.

[25] Wyszecki G, Stiles WS. Color science: concepts and methods, quantitative data and formulae. 2nd ed. New York: J. Wiley & Sons; 1982.

[26] Mortimer RJ, Graham KR, Grenier CRG, Reynolds JR. Influence of the film thickness and morphology on the colorimetric properties of spray-coated

electrochromic disubstituted 3,4-propylenedioxythiophene polymers. ACS Appl Mater Interfac 2009;1:2269–76.

**Figure legends**

**Fig. 1**

Particle size distribution, measured using a Malvern Zetamaster ZEM5002 colloid analyser, of a dilute colloidal suspension of RP formulated from an aqueous solution containing potassium hexacyanoruthenate(II) (0.5 mmol $dm^{-3}$), iron(III) chloride (0.5 mmol $dm^{-3}$), potassium chloride (35 mmol $dm^{-3}$), and ruthenium(III) chloride (0.020 mmol $dm^{-3}$) set at pH 2 with hydrochloric acid.

**Fig. 2**

RP film formation and scan rate studies on an ITO/glass substrate ($A$ = 2.8 $cm^2$). (a) Voltammetric cycles (every fifth scan shown), from an aqueous solution containing potassium hexacyanoruthenate(II) (0.5 mmol $dm^{-3}$), iron(III) chloride (0.5 mmol $dm^{-3}$), potassium chloride (35 mmol $dm^{-3}$), and ruthenium(III) chloride (0.020 mmol $dm^{-3}$) set at pH 2 with hydrochloric acid. The potential was held at +0.60 V for 5 s and then cycled, +0.60 V → −0.20 V → +0.60 V (*vs*. Ag/AgCl in 3.0 mol $dm^{-3}$ NaCl), 50 times at 50 $mVs^{-1}$. (b) Voltammetric cycles in an aqueous solution of potassium chloride (40 mmol $dm^{-3}$) at (1) 1 mV $s^{-1}$, (2) 2 mV $s^{-1}$, (3) 5 mV $s^{-1}$. (c) Cathodic peak current and (d) anodic peak current *vs*. scan rate for 1, 2, 5, 10, 20, 50, 100 and 200 mV $s^{-1}$.

**Fig. 3**

Scanning electron micrograph of a RP film on an ITO/glass substrate

**Fig. 4**

RP film formation on an ITO/glass substrate ($A$ = 2.8 $cm^2$). Voltammetric cycles (every fifth scan shown), from an aqueous solution containing potassium hexacyanoruthenate(II) (0.5 mmol $dm^{-3}$), iron(III) chloride (0.5 mmol $dm^{-3}$), potassium chloride (35 mmol $dm^{-3}$), and ruthenium(III) chloride (0.020 mmol $dm^{-3}$) set at pH 2 with hydrochloric acid. The potential was held at +0.60 V for 5 s and then cycled, +0.60 V → −0.20 V → +0.60 V (*vs*. Ag/AgCl in 3.0 mol $dm^{-3}$ NaCl), 100 times at 50 $mVs^{-1}$.

**Fig. 5**

(a) Following film formation as in Fig. 4, the cyclic voltammogram of RP on ITO/glass in 40 mmol $dm^{-3}$ KCl, +0.60 V → −0.20 V → +0.60 V, at 20 mV $s^{-1}$. (b) and (c) UV-visible absorbance spectra recorded every 1 s, in tandem with the cyclic voltammogram. The arrows indicate the direction of change in absorbance.

**Fig. 6**

(a) and (b) CIE 1931 *xy* chromaticity diagrams for reduction/oxidation of RP on ITO/glass in 40 mmol $dm^{-3}$ KCl. Data were calculated from the UV-visible absorbance data shown in Fig. 5. In Fig. 6 (b), the *xy* coordinates are plotted onto a diagram that shows the locus coordinates, with labelled hue wavelengths, and the evaluation of the complementary wavelength ($\lambda_c$) of the RP film.

**Fig. 7**

(a) Integrated plot (charge *vs.* potential) of the cyclic voltammogram, from Fig. 5 and (b) calculated relative luminance *vs.* potential for RP on ITO/glass in 40 mmol $dm^{-3}$ KCl. The arrows indicate the direction of the potential scan, starting at +0.60 V and scanning at 20 mV $s^{-1}$.

**Fig. 1**

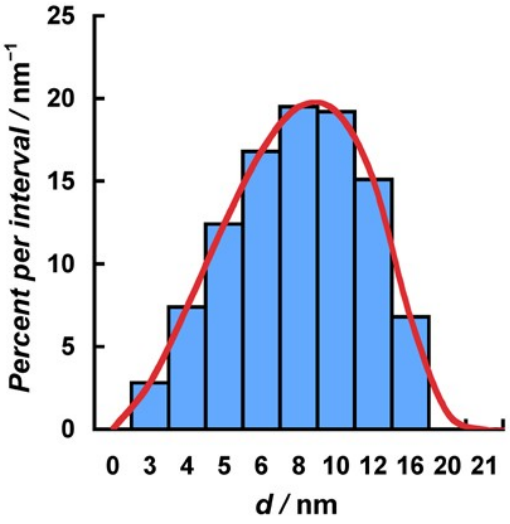
Percent per interval / nm⁻¹
25
20
15
10
5
0
0 3 4 5 6 8 10 12 16 20 21
d / nm

**Fig. 2**

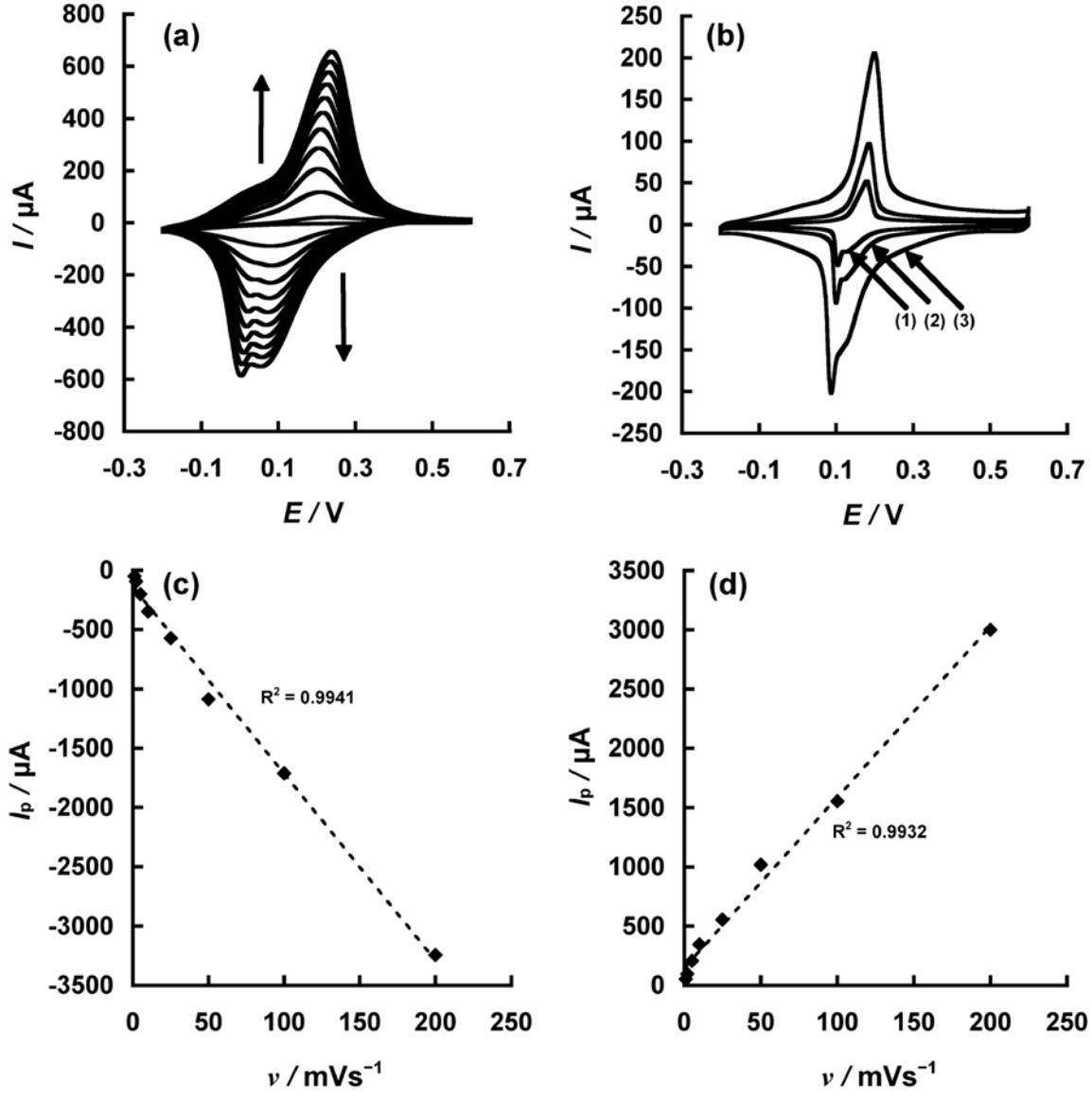

**Fig. 3**

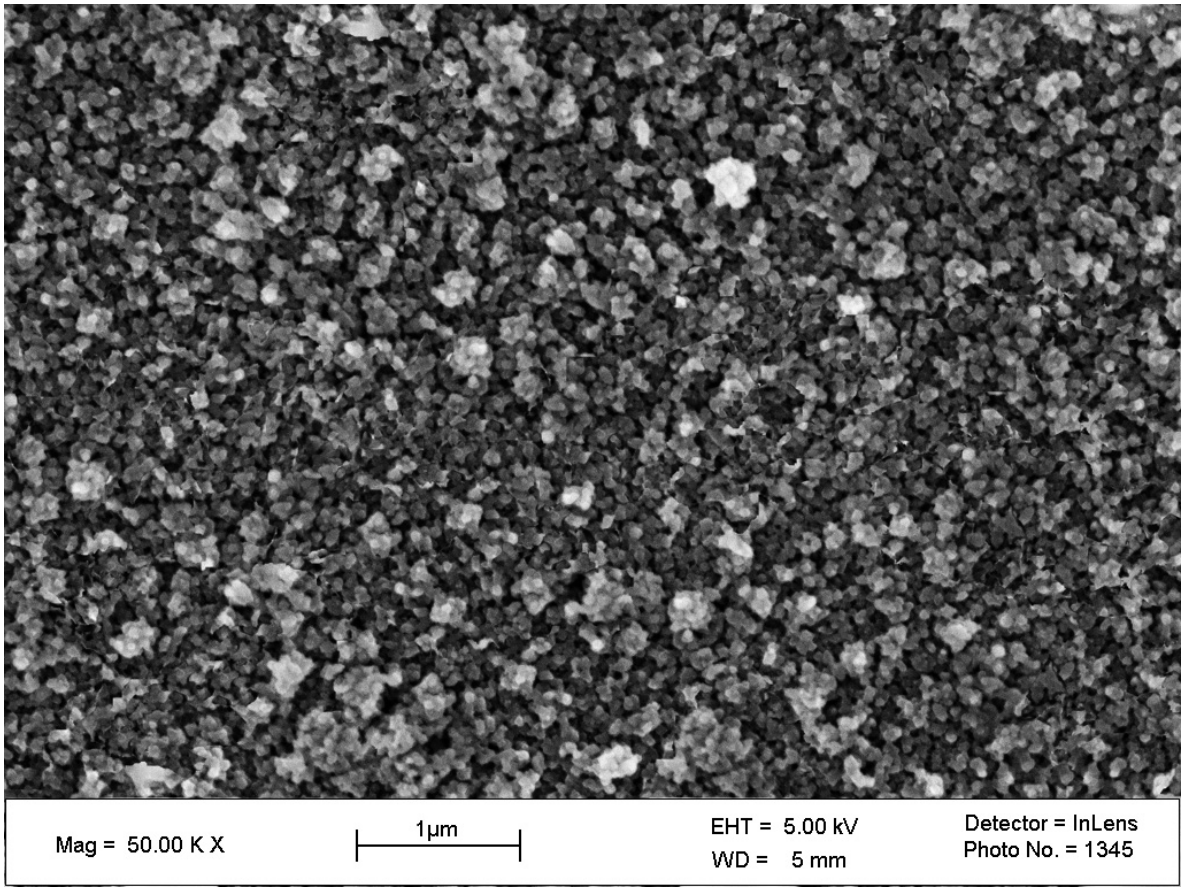
Mag = 50.00 K X
1µm
EHT = 5.00 kV
WD = 5 mm
Detector = InLens
Photo No. = 1345

**Fig. 4**

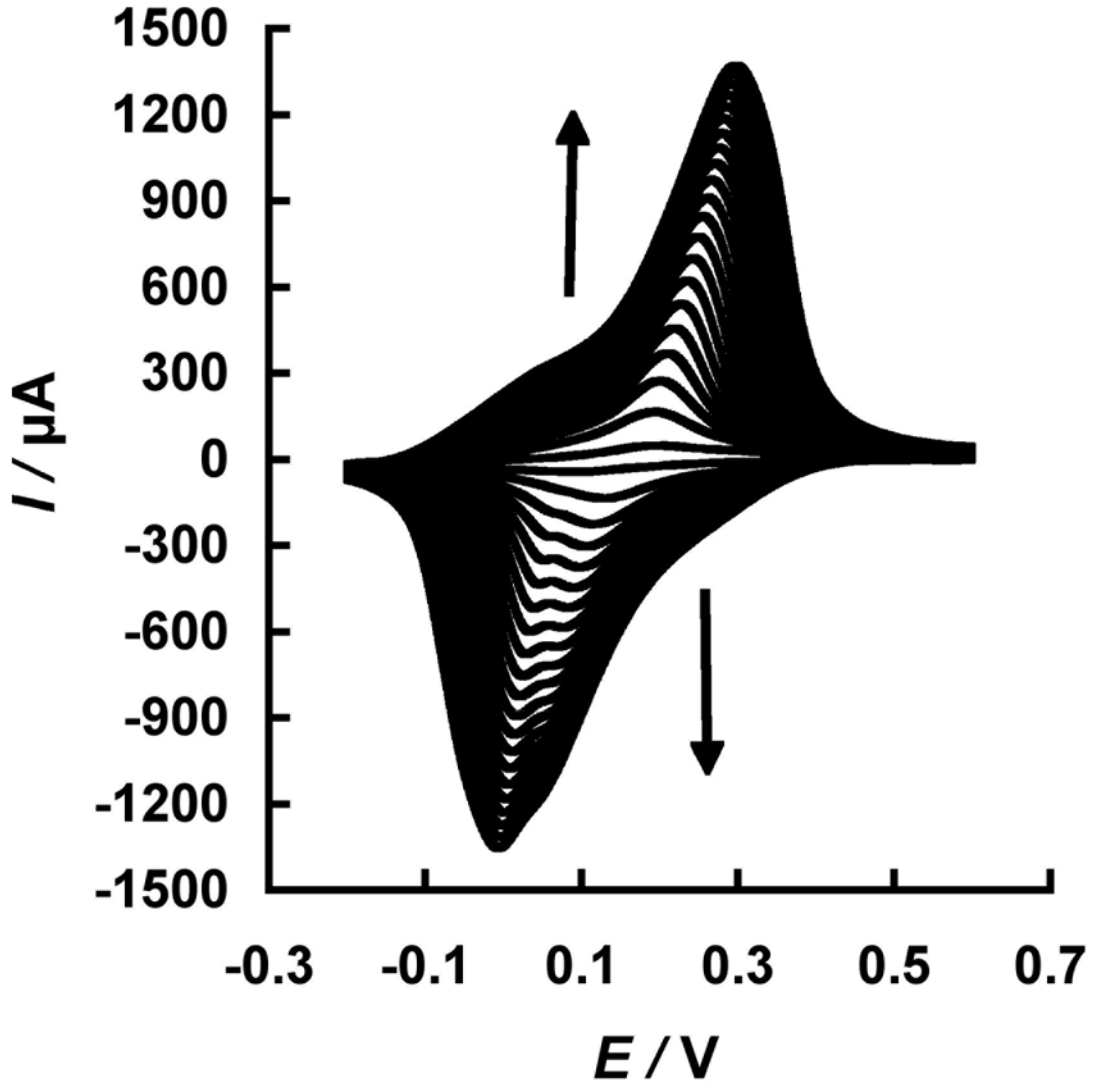
1500
1200
900
600
300
0
-300
-600
-900
-1200
-1500
I / μA
-0.3
-0.1
0.1
0.3
0.5
0.7
E / V

**Fig. 5**

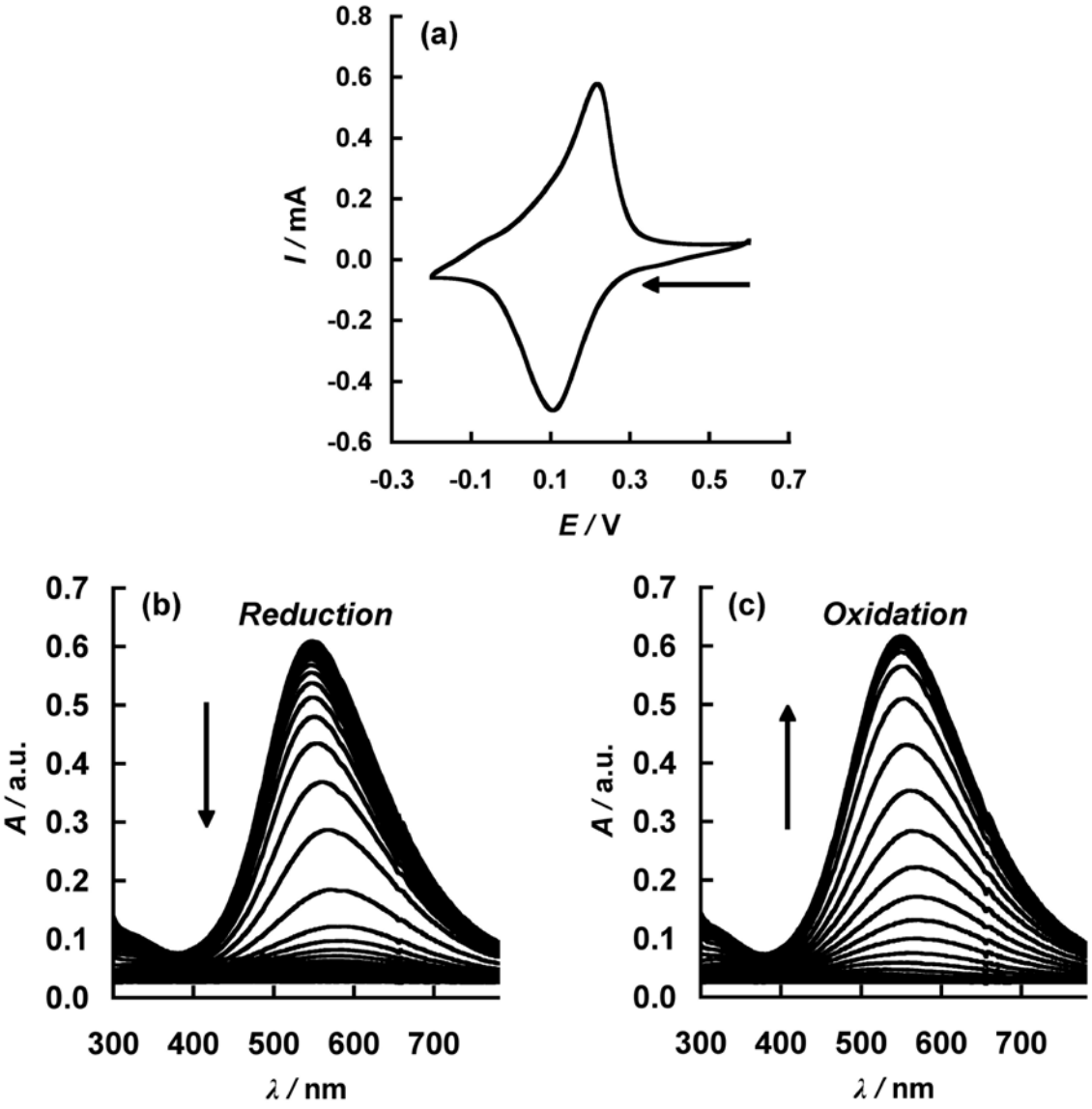

**Fig. 6**

**(a)**

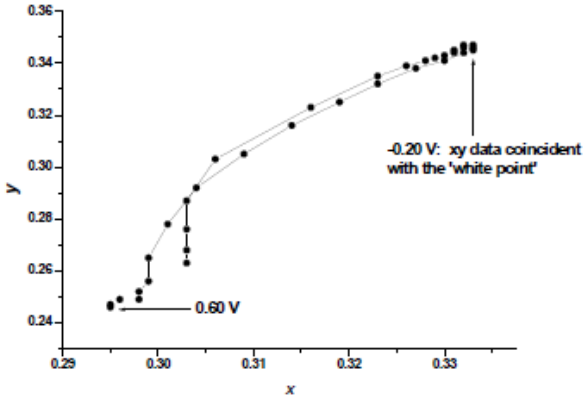
-0.20 V: xy data coincident
with the 'white point'
0.60 V
y
x

**(b)**

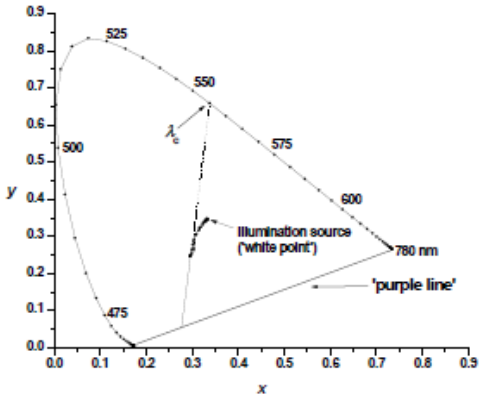
525
550
575
600
500
475
780 nm
Illumination source
('white point')
'purple line'
y
x

**Fig. 7**

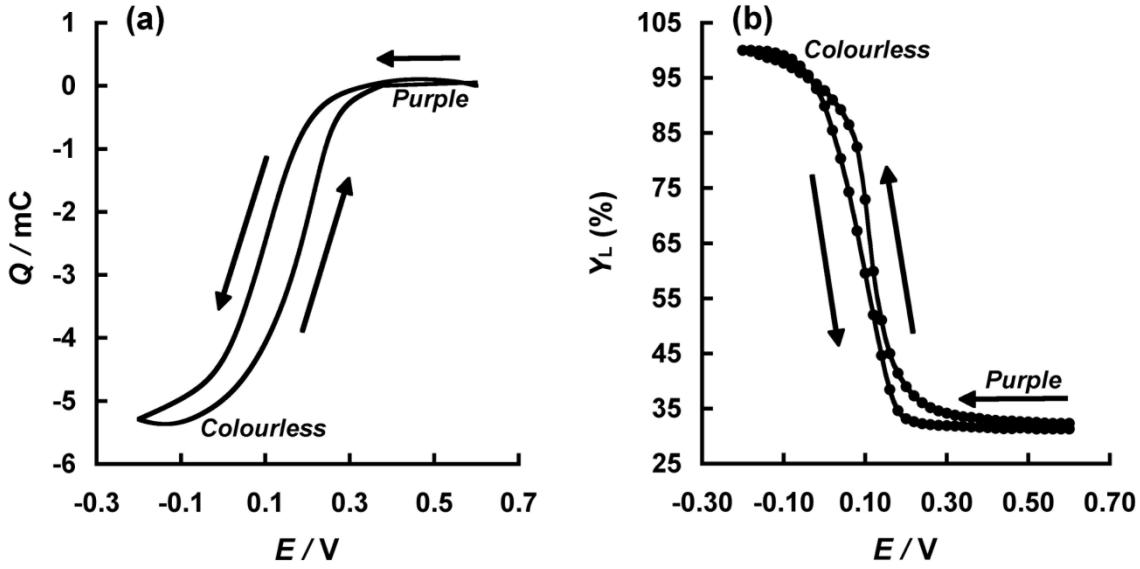
(a)
Purple
Colourless
Q / mC
E / V
1
0
-1
-2
-3
-4
-5
-6
-0.3
-0.1
0.1
0.3
0.5
0.7
(b)
Colourless
Purple
$Y_L$ (%)
E / V
105
95
85
75
65
55
45
35
25
-0.30
-0.10
0.10
0.30
0.50
0.70

**Table 1**

Numerical chromaticity coordinates for the electrochemical reduction and re-oxidation of a RP thin-film (5 mC $cm^{-2}$), at an ITO/glass electrode, in an aqueous solution containing potassium chloride (40 mmol $dm^{-3}$). Data were calculated using the spectral power distribution of a $D_{55}$ light source. The *xy* coordinates in bold are plotted in Fig. 6. The $\%Y_L$ data are plotted in Fig. 7 (b).

| *E*/V *vs.* Ag/AgCl | $\%Y_L$ | *x* | *y* | *L** | *a** | *b** |
|---|---|---|---|---|---|---|
| 0.60 | 32.3 | **0.295** | **0.246** | 64 | 27 | -36 |
| 0.58 | 32.3 | 0.295 | 0.246 | 64 | 27 | -36 |
| 0.56 | 32.3 | 0.295 | 0.247 | 64 | 26 | -36 |
| 0.54 | 32.4 | 0.295 | 0.247 | 64 | 26 | -36 |
| 0.52 | 32.5 | 0.296 | 0.247 | 64 | 27 | -36 |
| 0.50 | 32.6 | 0.296 | 0.248 | 64 | 26 | -35 |
| 0.48 | 32.6 | 0.297 | 0.248 | 64 | 27 | -35 |
| 0.46 | 32.8 | 0.297 | 0.248 | 64 | 27 | -35 |
| 0.44 | 32.8 | 0.297 | 0.248 | 64 | 27 | -35 |
| 0.42 | 32.8 | 0.298 | 0.249 | 64 | 27 | -35 |
| 0.40 | 33.0 | **0.298** | **0.249** | 64 | 27 | -35 |
| 0.38 | 33.2 | 0.299 | 0.250 | 64 | 27 | -35 |
| 0.36 | 33.4 | 0.299 | 0.250 | 64 | 27 | -35 |
| 0.34 | 33.5 | 0.300 | 0.251 | 65 | 27 | -34 |
| 0.32 | 33.8 | 0.300 | 0.252 | 65 | 26 | -34 |
| 0.30 | 34.2 | 0.301 | 0.252 | 65 | 27 | -34 |
| 0.28 | 34.6 | 0.301 | 0.254 | 65 | 26 | -33 |
| 0.26 | 35.2 | 0.302 | 0.255 | 66 | 26 | -33 |
| 0.24 | 36.1 | 0.302 | 0.257 | 67 | 25 | -33 |
| 0.22 | 37.3 | 0.302 | 0.260 | 67 | 24 | -32 |
| 0.20 | 39.0 | **0.303** | **0.263** | 69 | 23 | -31 |
| 0.18 | 41.4 | **0.303** | **0.268** | 70 | 21 | -30 |

| | | | | | | |
|---|---|---|---|---|---|---|
| 0.16 | 45.0 | **0.303** | **0.276** | 73 | 18 | -28 |
| 0.14 | 51.0 | **0.303** | **0.287** | 77 | 13 | -25 |
| 0.12 | 59.9 | **0.306** | **0.303** | 82 | 8 | -20 |
| 0.10 | 73.0 | **0.316** | **0.323** | 88 | 3 | -12 |
| 0.08 | 82.5 | **0.323** | **0.335** | 93 | 1 | -6 |
| 0.06 | 86.5 | **0.326** | **0.339** | 95 | 1 | -4 |
| 0.04 | 89.2 | **0.328** | **0.341** | 96 | 1 | -3 |
| 0.02 | 91.1 | **0.329** | **0.342** | 96 | 1 | -3 |
| 0.00 | 92.7 | **0.330** | **0.343** | 97 | 1 | -2 |
| −0.02 | 93.9 | **0.331** | **0.344** | 98 | 1 | -1 |
| −0.04 | 95.0 | **0.331** | **0.345** | 98 | 0 | -1 |
| −0.06 | 96.0 | **0.331** | **0.345** | 98 | 0 | -1 |
| -0.08 | 96.9 | **0.332** | **0.346** | 99 | 0 | 0 |
| −0.10 | 97.7 | **0.332** | **0.346** | 99 | 0 | 0 |
| −0.12 | 98.3 | 0.332 | 0.347 | 99 | 0 | 0 |
| −0.14 | 98.7 | 0.332 | 0.347 | 99 | 0 | 0 |
| −0.16 | 99.2 | 0.332 | 0.347 | 100 | 0 | 0 |
| −0.18 | 99.8 | 0.332 | 0.347 | 100 | 0 | 0 |
| −0.20 | 100.0 | **0.332** | **0.347** | 100 | 0 | 0 |
| −0.18 | 100.0 | 0.332 | 0.347 | 100 | 0 | 0 |
| −0.16 | 99.9 | 0.332 | 0.347 | 100 | 0 | 0 |
| −0.14 | 99.9 | 0.332 | 0.347 | 100 | 0 | 0 |
| −0.12 | 99.5 | 0.333 | 0.347 | 100 | 1 | 0 |
| −0.10 | 99.1 | **0.333** | **0.347** | 100 | 0 | 0 |
| −0.08 | 98.4 | **0.333** | **0.347** | 99 | 0 | 0 |
| −0.06 | 97.2 | **0.333** | **0.346** | 99 | 1 | 0 |
| −0.04 | 95.5 | **0.333** | **0.345** | 98 | 1 | -1 |
| −0.02 | 93.0 | **0.332** | **0.344** | 97 | 1 | -1 |
| 0.00 | 89.9 | **0.330** | **0.341** | 96 | 2 | -3 |
| 0.02 | 85.5 | **0.327** | **0.338** | 94 | 2 | -4 |

| | | | | | | |
|---|---|---|---|---|---|---|
| 0.04 | 80.4 | **0.323** | **0.332** | 92 | 3 | -7 |
| 0.06 | 74.3 | **0.319** | **0.325** | 89 | 4 | -10 |
| 0.08 | 67.3 | **0.314** | **0.316** | 86 | 6 | -14 |
| 0.10 | 59.5 | **0.309** | **0.305** | 82 | 8 | -19 |
| 0.12 | 52.0 | **0.304** | **0.292** | 77 | 11 | -23 |
| 0.14 | 44.7 | **0.301** | **0.278** | 73 | 16 | -27 |
| 0.16 | 38.4 | **0.299** | **0.265** | 68 | 21 | -31 |
| 0.18 | 34.6 | **0.299** | **0.256** | 65 | 24 | -33 |
| 0.20 | 33.1 | **0.298** | **0.252** | 64 | 25 | -34 |
| 0.22 | 32.6 | 0.298 | 0.251 | 64 | 26 | -34 |
| 0.24 | 32.2 | 0.298 | 0.250 | 64 | 26 | -34 |
| 0.26 | 32.1 | 0.297 | 0.250 | 63 | 26 | -34 |
| 0.28 | 32.0 | 0.297 | 0.250 | 63 | 26 | -34 |
| 0.30 | 31.9 | 0.297 | 0.249 | 63 | 26 | -35 |
| 0.32 | 31.9 | 0.297 | 0.249 | 63 | 26 | -35 |
| 0.34 | 31.8 | 0.297 | 0.249 | 63 | 26 | -35 |
| 0.36 | 31.7 | 0.296 | 0.249 | 63 | 26 | -35 |
| 0.38 | 31.6 | 0.296 | 0.249 | 63 | 26 | -35 |
| 0.40 | 31.6 | **0.296** | **0.249** | 63 | 26 | -35 |
| 0.42 | 31.4 | 0.296 | 0.249 | 63 | 26 | -35 |
| 0.44 | 31.4 | 0.296 | 0.248 | 63 | 26 | -35 |
| 0.46 | 31.4 | 0.296 | 0.248 | 63 | 26 | -35 |
| 0.48 | 31.5 | 0.296 | 0.247 | 63 | 27 | -35 |
| 0.50 | 31.4 | 0.296 | 0.247 | 63 | 26 | -35 |
| 0.52 | 31.3 | 0.296 | 0.247 | 63 | 26 | -35 |
| 0.54 | 31.3 | 0.295 | 0.246 | 63 | 27 | -36 |
| 0.56 | 31.3 | 0.295 | 0.246 | 63 | 27 | -36 |
| 0.58 | 31.3 | 0.295 | 0.247 | 63 | 26 | -35 |
| 0.60 | 31.3 | **0.295** | **0.247** | 63 | 26 | -35 |